Quantum Electronics **46** (8) 719–725 (2016)

NONLINEAR OPTICAL PHENOMENA DOI: 10.1070/QEL16026

Z-scanning under monochromatic laser pumping: a study of saturatable absorption in a suspension of multiwalled carbon nanotubes

G.M. Mikheev, R.Yu. Krivenkov, K.G. Mikheev, A.V. Okotrub, T.N. Mogileva

Abstract. **A system has been developed and designed based on a single-mode single-frequency passive *Q*-switched pulsed YAG : Nd^{3+} laser to investigate with high accuracy the nonlinear optical properties of a liquid placed in an optical cell with uncoated input windows. The efficiency of this system is demonstrated by examples of studying the saturable absorption of an aqueous suspension of multiwalled carbon nanotubes and the nonlinear absorption of a colour glass filter ZhS18 at a wavelength of 532 nm.**

Keywords: *z-scan technique, monochromatic laser pumping, interference, reflection, saturable absorption, nonlinear bleaching and absorption, multiwalled carbon nanotubes, colour glass filter.*

1. Introduction

One of the methods for studying the nonlinear optical properties of materials is the *z*-scan technique, which is based on measuring the optical transmittance of a sample under study when scanning it along the axis of a focused laser beam. This method has been known for a long time [1, 2]. Currently, it is widely applied to investigate the optical limiting and nonlinear bleaching of suspensions of different nanoparticles using nano- and femtosecond lasers (see, e.g., [3–11]). The *z*-scan technique provides information about nonlinear transmittance and nonlinear refraction coefficients. The *z*-scan scheme with an open aperture is generally used to measure the nonlinear transmittance [12], whereas the scheme with a closed aperture is applied to study nonlinear refraction. There are *z*-scan schemes in which measurements with open and closed apertures are performed in one scan pass [13, 14]. To this end, the laser beam transmitted through a sample is split into two beams; these beams are directed to photodetectors, one of which is equipped with an input aperture.

When carrying out *z*-scan measurements of a sample with uncoated input surfaces using a single-frequency laser source, the optical reflection coefficient of the sample may randomly change. The reason is a stepwise change in the frequency of the longitudinal laser mode, which distorts the interference pattern of reflected beams from the front and rear sample surfaces.

In addition, when carrying out *z*-scan measurements, an error in aligning the coordinate table motion direction with the laser beam axis leads to a small displacement of the laser beam in the lateral direction with respect to the sample. As a result, when scanning a sample along the focused laser beam axis, the optical path of the beam reflected from the rear sample surface may slightly change because of the deviation of the sample surfaces from plane parallelism.

As a consequence, in the case of *z*-scan measurements under monochromatic pumping, the sample reflectance may significantly change due to the interference of the beams reflected from the front and rear sample surfaces. This change may lead to variations (within few percent) in the measured signal characterising the transmittance of a sample having no nonlinear optical properties.

To reduce the influence of the interference on the measurement results, antireflection coatings should be deposited on the sample surfaces. According to [2], to reduce the transmittance modulation to 1%, the reflectances of the face and rear sides of a sample should not exceed 0.25%. In some cases it is not expedient to deposit antireflection coatings (characterised by a relatively low beam strength), because a sample is exposed to high-intensity laser radiation during *z*-scan measurements when a focused laser beam passes through the waist. In addition, when analysing the nonlinear optical properties of a sample in a wide wavelength range, it is rather difficult to provide a low reflectance of its surfaces in the entire wavelength range under study.

Thus, the existence of experimental errors caused by the interference of reflected beams from uncoated sample surfaces under monochromatic laser pumping complicates the study of fine nonlinear optical effects, which are accompanied by a slight variation in the sample transmittance. An example of these effects is saturable absorption (SA): bleaching of an optical medium, which is characterised by a short-term decrease in its absorption coefficient when a high-intensity light pulse passes through it; this effect is caused by an electron transition between two energy levels. Recently, researchers designing mode-locked lasers have paid much attention the SA manifesting itself in nanocarbon materials [15–19].

The purpose of this study was to develop and design a *z*-scan system that would make it possible to obtain with high accuracy the dependences of nonlinear transmittance and nonlinear refraction of a liquid placed in an optical cell with uncoated input windows on the coordinate *z* in one scan pass under single-frequency laser pumping and to demonstrate the efficiency of this system by an example of detecting SA in an aqueous suspension of multiwalled carbon nanotubes and

G.M. Mikheev, R.Yu. Krivenkov, K.G. Mikheev, T.N. Mogileva
Institute of Mechanics, Ural Branch, Russian Academy of Sciences, ul. T. Baramzinoi 34, 426067 Izhevsk, Russia;
e-mail: mikheev@udman.ru, roman@udman.ru;
A.V. Okotrub A.V. Nikolaev Institute of Inorganic Chemistry, Siberian Branch, Russian Academy of Sciences, prosp. Akad. Lavrent'eva 3, 630090 Novosibirsk, Russia

Received 4 February 2016; revision received 9 June 2016
Kvantovaya Elektronika **46** (8) 719–725 (2016)
Translated by Yu.P. Sin'kov

nonlinear absorption in a colour glass filter ZhS18 at a wavelength of 532 nm.

2. Preliminary estimates

Generally, when experimentally studying the nonlinear optical properties of a nanocarbon material suspension, the latter is placed in an optical cell with plane-parallel working surfaces. In z-scan measurements, the cell is located on a single-axis table so as to orient the cell working surface with respect to the incident beam at an angle close to normal; i.e., the beam is incident on the cell surface at a small angle φ. When calculating the laser beam transmittance through the cell with nanoparticle suspension, one can neglect the reflections from the cell inner surface, because the refractive indices of glass (quartz) and liquid (for example, water) have close values. For simplicity, we also neglect the light absorption in the suspension. Then transmittance T of a monochromatic laser beam through a cell with a suspension can be determined in the first approximation using the multipath interference occurring during light wave transmission through the plane-parallel dielectric layer under study. To this end, we will use the well-known Airy formula (see, for example, [20]):

$$T = \frac{1}{1 + [4r/(1-r)^2]\sin^2(\delta/2)}, \tag{1}$$

$$\delta = (4\pi/\lambda)nd\cos\varphi \pm \pi, \tag{2}$$

where r is the reflectance from the layer boundaries; λ is the radiation wavelength; and n and d are, respectively, the refractive index and thickness of the dielectric layer. It is well known that $r = 0.04$ for the air–glass (quartz) interface under normal incidence. It follows from formulas (1) and (2) that a small shift of the incident radiation wavelength, which is possible because of the variation in the laser frequency by $\sim$0.01 cm^{-1}, may change the transmittance by 1.1%. The same occurs with an insignificant variation in the dielectric layer thickness. For example, if the change in the dielectric layer thickness (caused by the error in aligning the optical system and the cell tapering) in z-scan measurements is 0.02 μm, the transmittance may change by 2.5%. Thus, under monochromatic laser pumping, the interference of the beams reflected from the face and rear sides of a plane-parallel cell with a suspension may lead to a change in transmittance, which is in no way related to the suspension nonlinearity but is due to the laser frequency instability and the optical-cell imperfection.

3. A z-scan system with a single-frequency laser source

One of the ways to exclude the influence of the interference on the transmittance of an optical cell with a liquid in z-scan measurements is to use a narrow laser beam and incline the optical cell with respect to the incident beam. In this case, one can provide conditions under which the beams reflected from the face and rear sides of the cell do not interfere.

A simplified optical scheme of the developed and designed z-scan system is presented in Fig. 1. An YAG:Nd^{3+} laser with a cavity designed in correspondence with the optical scheme described in [21] was used as a single-frequency laser source (*1*). The optical cavity length was about 110 cm. The laser operated in the single-mode and single-frequency regimes to generate smooth 1064-nm pulses with a duration of 21.2 ns. The laser-beam diameter was 1.7 mm. Parameter M^2, which characterises the laser beam quality, was measured using a lens with a focal length of 0.192 m and a BC 106-VIS (ThorLabs) laser beam profilometer to be 1.03.

The laser beam passed through IR filter (*2*) was directed [using rotational mirror (*3*)] to a second-harmonic converter, composed of half-wave plate (*4*), nonlinear optical crystal (*5*), and filter (*6*) (absorbing at the fundamental frequency). At a wavelength of 532 nm, laser pulse duration τ, measured (at the level of 0.5 of the intensity maximum) using an SIR-5 photodetector (ThorLabs) with an operating speed of about 60 ps and a broadband TDS7704B digital oscilloscope (TEKTRONIX) with a transmission band of 7 GHz, was 13.6 ns, and the laser-beam diameter, measured at the level of 1/e^2 of the intensity peak, was 1.3 mm. Then the second-harmonic radiation was directed to optical splitter (*7*), installed at an angle of incidence of 45°. The thickness of plate (*7*) was chosen so as to separate in space the laser beams reflected from its face and rear sides. This measure excludes the inter-

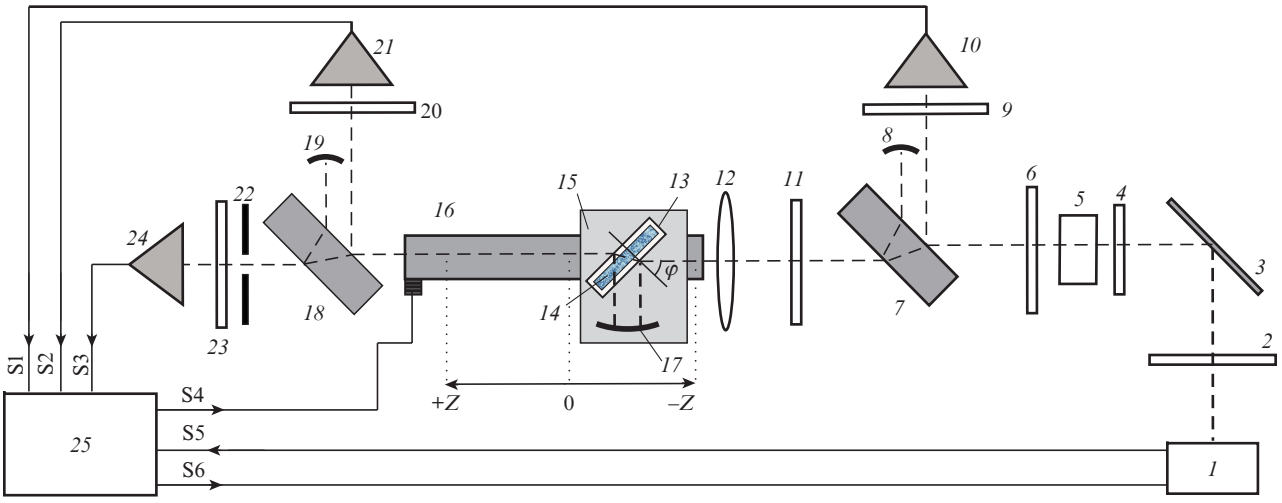

Figure 1. Schematic of the experiment.

ference of the reflected beams and provides a constant reflectance from the aforementioned surfaces at a stepwise change in the longitudinal mode of the laser cavity. The beam reflected from the front plate surface of (*7*), after weakening by neutral filter (*9*), arrived at reference photodetector (*10*), which measured energy E_{in} of incident laser pulses. Photodetector (*10*) was calibrated using pyroelectric ES111 energy meter through a PM100USB interface (ThorLabs). The beam reflected from the rear side of plate (*7*) was absorbed by screen (*8*).

To carry out *z*-scan measurements, the laser beam transmitted through neutral filters (*11*) was focused by lens (*12*) with a focal length of 0.192 m and directed to plane-parallel optical cell (*13*) with suspension (*14*), mounted on platform (*15*) of LTS 150/M single-axis table (*16*) (ThorLabs), with a minimum positioning step of 25 μm. The platform motion axis was aligned parallel to the laser beam optical axis. The suspension layer thickness was 1.055 mm, and the cell wall thickness was 3 mm. Thus, the total cell thickness was about 7 mm. The optical cell was installed either perpendicular to the incident beam ($\varphi = 0$) or at an angle of $\varphi = 45°$ with respect to it. At $\varphi = 45°$ (see Fig. 1), the laser beams reflected from the face and rear sides of the cell were not intersected in space and, therefore, did not interfere. These beams were absorbed by screen (*17*), mounted on the platform. The absence of interference provided constant reflectances from the external surfaces of the optical cell, independent of the cell position on the *z* axis and a stepwise change in the longitudinal mode of laser cavity.

After passing through the optical cell, the laser beam was partially directed [due to the reflection from the face surface of thick optical plate (*18*)] to photodetector (*21*), which was used to measure nonlinear optical transmittance T_{oa} in the open-aperture regime according to the formula $T_{oa} = E_{out,oa}/E_{in}$, where $E_{out,oa}$ is the laser pulse energy measured by photodetector (*21*). The beam reflected from the rear surface of splitter (*18*) was absorbed by screen (*19*), and neutral filter (*20*) served to reduce the radiation intensity. After the splitter, the main laser beam passed through aperture (*22*) (attenuation coefficient $S = 0.45$) and neutral filters (*23*) to arrive at photodetector (*24*), which was used to determine nonlinear transmittance T_{ca} in the closed-aperture regime according to the formula $T_{ca} = E_{out,ca}/E_{in}$, where $E_{out,ca}$ is the laser pulse energy measured by photodetector (*24*). The automatic measurement of laser pulse energies E_{in}, $E_{out,oa}$, and $E_{out,ca}$ and the control of the laser and single-axis-table step motor operation were performed using specially developed computer-aided unit (*25*) and special software [22] through communication channels S1, S2, …, S6, as is shown in Fig. 1. The aforementioned software makes it possible to take into account only the laser shots in which laser pulse energy E_{in} satisfies the condition

$$(1 - k)E_{in,aver} < E_{in} < (1 + k)E_{in,aver}, \quad (3)$$

where $k \ll 1$, and $E_{in,aver}$ is the laser pulse energy obtained by averaging over no less than 100 laser shots. The software in use makes it possible to change the k value. In all the experiments described below, $k = 0.1$.

4. Testing of the *z*-scan system

To test the developed *z*-scan system, we performed comparative experiments on measuring transmittance T_{oa} of an optical cell filled with distilled water, oriented perpendicular ($\varphi = 0$) and obliquely ($\varphi = 45°$) with respect to the incident laser beam. The measurements performed at a fixed *z* value showed that normalised transmittances $\overline{T}_{oa}$ for $\varphi = 45°$ and $\overline{T}_{oa}$ ($\varphi = 0$), obtained by averaging over 30 laser pulses satisfying condition (3), lie in the ranges of $(1 - \delta_1, 1 + \delta_1)$ and $(1 - \delta_2, 1 + \delta_2)$, respectively, where $\delta_1 = 0.0015$ and $\delta_2 = 0.0033$. This means that the measurement error for the cell oriented at $\varphi = 45°$ is smaller by a factor of 2.2 than for $\varphi = 0$. Figure 2 shows dependences of normalised transmittances $\overline{T}_{oa}$ on coordinate *z*, where each point was obtained by averaging over 30 laser pulses satisfying condition (3). It can be seen that the ordinates of points in dependences (*1*) and (*2*) lie in the ranges of $(1 - \Delta_1, 1 + \Delta_1)$ and $(1 - \Delta_2, 1 + \Delta_2)$, respectively, where $\Delta_1 = 0.0018$ and $\Delta_2 = 0.011$. Thus, when the cell is scanned along the *z* axis, the error in measuring the transmittance increases; note that, for the experimental dependence obtained at $\varphi = 0$, the error is larger by a factor of about 6 than for $\varphi = 45°$. This is a clear evidence of the possibility of reducing the error in measuring the transmittance by applying a narrow laser beam and orienting the cell with a liquid under study obliquely with respect to the incident laser beam.

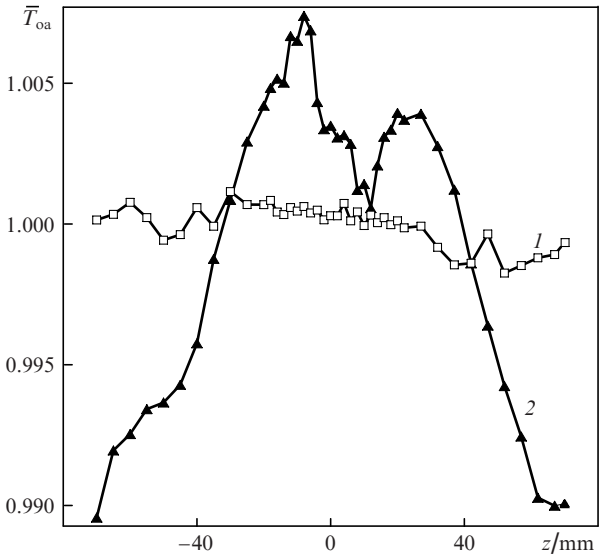

Figure 2. Dependences of normalised transmittance $\overline{T}_{oa}$ of a cell with distilled water on coordinate *z*, recorded at $\varphi =$ (*1*) 45° and (*2*) 0.

5. Application of the developed system to study the saturable absorption in a suspension of multiwalled carbon nanotubes

The *z*-scan system developed by us was used to observe and study the SA in an aqueous suspension of multiwalled carbon nanotubes (CNTs), synthesised by electric-arc evaporation of graphite [23]. To obtain an aqueous suspension, synthesised CNTs were purified and chemically modified according to the technique described in [24, 25]. Multiwalled CNTs of the highest quality were found in an excrescence of transferred carbon during electric-arc evaporation of graphite in an inert atmosphere. They do not contain any impurities of other elements, have a minimum number of structural defects, and exhibit ballistic electrical conductivity. To make the nanotubes synthesised by electric-arc method able of forming a stable suspension in water and to purify CNTs from nanopar-

ticles of amorphous carbon, nanographite, and glassy carbon, the inner part of the transferred carbon excrescence was subjected to chemical treatment.

CNTs were purified from minor synthesis products on the assumption that different carbon phases differently interact with a solution of potassium permanganate ($KMnO_4$) in a concentrated sulfuric acid (H_2SO_4). The interaction of graphite with Mn_2O_7 formed in the solution leads to the synthesis of a layered intercalated compound: graphite oxide with a composition similar to C_4O. Under the same conditions, amorphous carbon decays with the formation of organic compound: mellitic acid $C_6(COOH)_6$, which can easily be dissolved in water. The oxidation of multiwalled CNTs leads to the attachment of oxygen-containing groups to the surface of particles, thus providing the formation of a colloidal CNT solution in water.

CNTs were precipitated using a solution of ferric chloride $FeCl_3$. Iron hydroxide was released as a result of the hydrolysis to form a composite with oxidised CNTs. A small amount of concentrated hydrochloric acid was added to the composite dried in air, and then the mixture was kept for 24 h to implement iron hydroxide dissolution. The $FeCl_3$ residue was removed from the precipitate by washing on a filter, first with a 5% solution of hydrochloric acid to a colourless filtrate and then with distilled water (until the filtrate acquired a dark colour). A structural study of the suspension nanoparticles using a JEOL JSM-6700F scanning electron microscope showed that most of CNTs have a diameter of 15–20 nm and a length less than 1 μm (Fig. 3) [26].

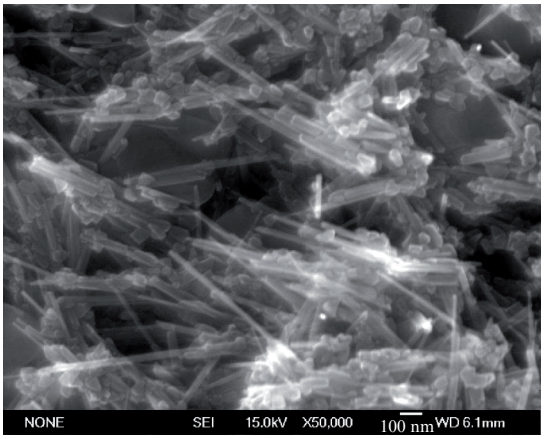

Figure 3. Scanning electron microscopy image of nanoparticles in the suspension under study.

Figure 4 shows the optical density spectra of the suspension at different CNT concentrations (with respect to the spectrum of distilled water), obtained with a double-beam Lambda 650 UV spectrometer. A typical Raman spectrum of multiwalled CNTs deposited from the suspension onto a glass substrate is shown in Fig. 5. The spectrum was recorded with a Raman spectrometer (Horiba Jobin Yvon HR800) at an excitation wavelength of 632.8 nm and a power density of 5 kW cm^{-2}. This spectrum contains graphite modes with frequency shifts of 1585 cm^{-1} (G band, which is due to the in-plane vibrations of C – C bonds) and 1336 cm^{-1} (D band, which is due to the presence of defects in nanotubes) [27, 28]. The spectrum contains also a mode with a frequency shift of 2660 cm^{-1} (2D band), which is related to the two-photon scattering [28]. The high intensity of the D band and the low intensity of the 2D band with respect to the G band indicate the presence of a large number of defects in the nanotubes under study [27].

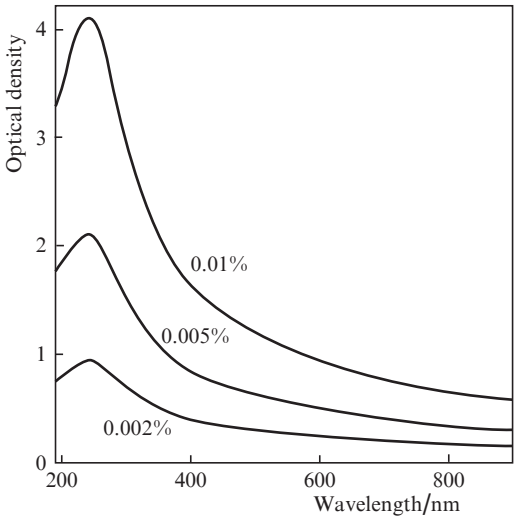

Figure 4. Optical density spectra of suspensions of multiwalled CNTs with concentrations of 0.01, 0.005, and 0.002 wt%.

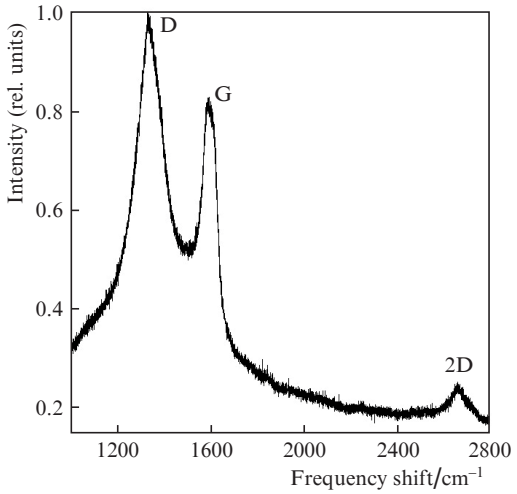

Figure 5. Raman spectrum of multiwalled CNTs, obtained upon excitation by light at a wavelength of 632.8 nm and a power density of 5 kW cm^{-2}.

To study the nonlinear optical properties, a CNT suspension with a concentration of 0.01 wt% was placed in a standard plane-parallel optical cell with a working thickness of 1.055 mm and walls 3-mm-thick each. When carrying out z-scan measurements, the cell was installed at an angle $\varphi = 45°$ with respect to the optical axis of the focused laser beam (see Fig. 1). The laser-pulse repetition rate was 1 Hz. Figure 6 shows the dependences of normalised nonlinear transmittance $\overline{T}_{oa}(z) = T_{oa}(z)/T_{oa}$ (z = 70 mm), obtained for laser pulse energies E_{in} = 11, 28, 49, and 181 μJ. The experimental data for $T_{ca}(z)$ and $T_{oa}(z)$ at E_{in} = 11 μJ were used to obtain the dependence of normalised transmittance $\bar{t}(z) = t(z)/t(z = 70$ mm), where $t(z) = T_{ca}(z)/T_{oa}(z)$ (Fig. 7). In accordance with [12], this dependence characterises the third-order nonlinear refraction in the absence of nonlinear absorption. Note that the experi-

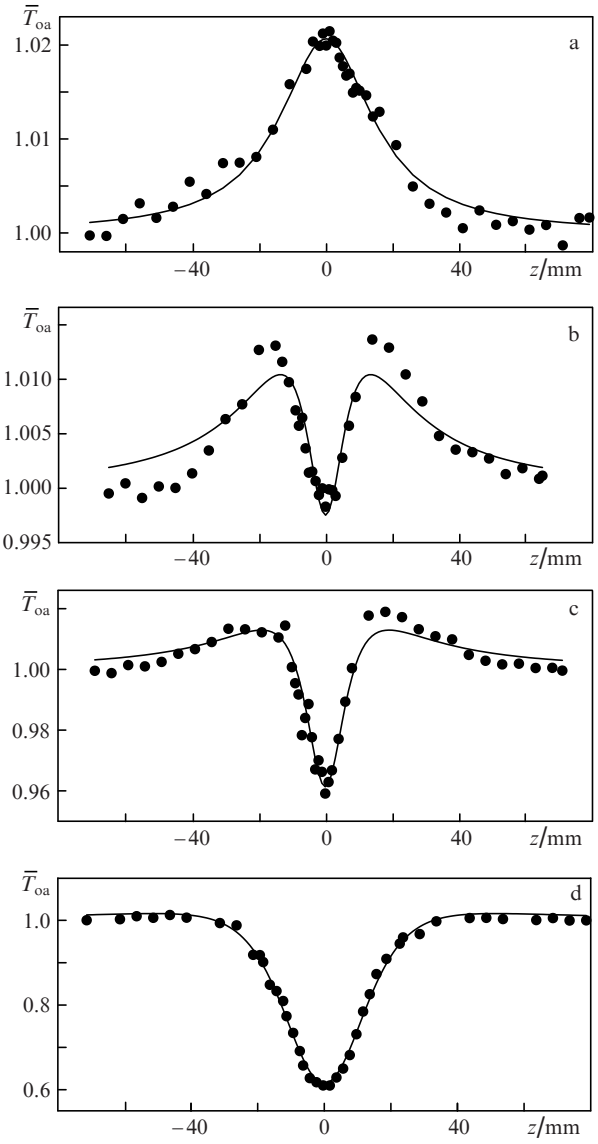

Figure 6. Dependence of normalised transmittance $\overline{T}_{oa}$ of an aqueous multiwalled CNT suspension with a concentration of 0.01 wt% on the coordinate z, obtained in the open-aperture experiment at $\varphi = 45°$ and E_{in} = (a) 11, (b) 28, (c) 49, and (d) 181 μJ (circles are experimental data and solid lines are approximations by theoretical functions).

mental values of $\bar{t}(z)$, obtained at E_{in} = 28, 49, and 181 μJ, have a large spread and cannot be interpreted as the result of nonlinear refraction.

The manifestation of the SA in the suspension under study is pronounced in Fig. 6a. It can be seen that, in the region of the beam waist ($z = 0$), where the incident radiation intensity is about 10 MW cm^{-2}, transmittance $\overline{T}_{oa}$ increases by about 2% in comparison with the linear transmittance. The dependence $\overline{T}_{oa}(z)$, obtained at E_{in} = 28 μJ (Fig. 6b), exhibits (along with SA) a dramatic decrease in $\overline{T}_{oa}$ in the waist region. The further increase in E_{in} (Figs 6c, 6d) is accompanied by a significant decrease in $\overline{T}_{oa}$ at $z = 0$. A possible mechanism leading to the reduction of $\overline{T}_{oa}$ at incident beam intensities exceeding 10 MW cm^{-2} is the two-photon absorption and (or) inverse SA [29].

The experimental dependences presented in Fig. 6 can be approximated using the following expression for absorption coefficient α, characterising SA [16], with allowance for the nonlinear absorption caused by two-photon absorption [2, 30]:

$$\alpha = \alpha_{ns} + \alpha_0/[1 + I(z)/I_{sat}] + \beta I(z), \quad (4)$$

where $I(z)$ is the incident beam intensity; α_{ns} is the linear absorption coefficient, which is not related to the SA; α_0 is the absorption coefficient characterising the SA at intensity $I(z)$ tending to zero; I_{sat} is the saturation intensity (coefficient determining the ability of a medium to exhibit self-bleaching); β is a coefficient characterising two-photon absorption; $I(z) = E_{in}/[\tau S(z)]$; $S(z) = \pi w^2(z)$; and $w(z)$ is the laser-beam radius at a distance of z from the waist ($z = 0$) of focused laser beam. A Gaussian beam obeys the relation $w^2(z) = w_0^2[1 + (\lambda z/\pi w_0^2)^2]$, where w_0 is the beam radius in the waist. In our experiments, w_0 was taken to be 51.3 μm.

When approximating the experimental data presented in Fig. 6a, the term describing the two-photon absorption in Eqn (4) can be neglected. As can be seen in Fig. 6a, the approximating curve with two found parameters, α_0 = 0.25 cm^{-1} and I_{sat} = 2.8 MW cm^{-2}, is in good agreement with the experimental dependence. With allowance for this fact, we find that α_{ns} = 24.9 cm^{-1}. An approximation of the experimental data presented in Fig. 6d yields β = 0.2 cm MW^{-1}. Some deviation of the values of the approximating functions presented in Figs 6b–6d from the experimental points can be explained by the manifestation of nonlinear light scattering [26, 31], which was disregarded in expression (4).

It is generally assumed that single-walled rather than multiwalled CNTs exhibit saturable absorption. This assumption is based on the discrete energy structure of single-walled CNTs, which results in absorption peaks at separate wavelengths [32–35]. However, the SA was also observed in multiwalled CNTs (see, for example, [36, 37]). It can be seen in Fig. 4 that the aqueous suspension studied by us has a smooth absorption spectrum without any distinctive peaks in a wide wavelength range, including the wavelength of 532 nm. This means that the SA, which was observed by us at this wavelength, may occur in a wide wavelength range. However, as can be seen in Figs 6b and 6c, the saturable absorption occurring in multiwalled CNTs is suppressed by two-photon absorption and nonlinear light scattering when the radiation intensity slightly increases. This fact indicates that multiwalled CNT are not promising elements for saturating absorbers.

It follows from the data in Fig. 7 that nonlinear refraction in a suspension of multiwalled CNTs is only slightly pronounced. The theoretical expressions describing the third-order nonlinear refraction [2] make it possible to approximate the experimental data presented in Fig. 7 and determine the Kerr nonlinearity index: $n_2 = -3.2 \times 10^{-6}$ cm^2 MW^{-1}. The modulus of the found n_2 value is close to the nonlinear refraction coefficient of a silicate glass composite with copper nanoparticles [38] and exceeds (by a factor of about 100) the n_2 value for carbon disulfide, obtained with nanosecond laser pulses [39]. The absence of regularity with minima and maxima (characteristic of nonlinear refraction) in the experimental dependences $\bar{t}(z)$ recorded at E_{in} = 28, 49, and 181 μJ can be explained by an increase in nonlinear light scattering with an increase in the incident beam power.

Note also that the dependences of nonlinear transmittance on z similar to our plots (see Fig. 6) were previously obtained by other researchers, who studied, in particular, the

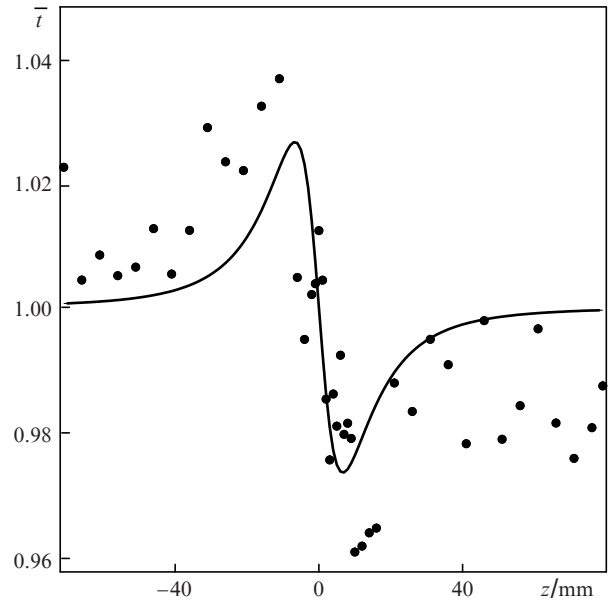

Figure 7. Dependence of normalised transmittance $\overline{t}$, characterising the nonlinear refraction of aqueous multiwalled CNT suspension, on the coordinate z, obtained at $\varphi = 45°$ and $E_{in} = 11$ μJ (circles are experimental data and the solid line is an approximation by theoretical function).

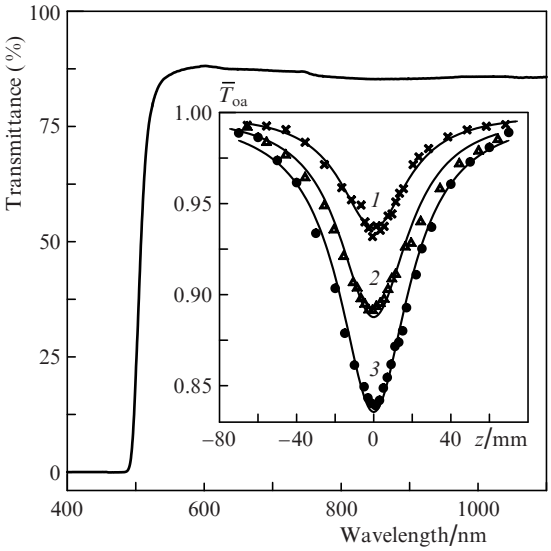

Figure 8. Dependence of the linear transmittance of a yellow glass filter ZhS18 at $\varphi = 45°$ on the light wavelength and (inset) the dependence of normalised nonlinear transmittance $\overline{T}_{oa}$ of the same filter on the coordinate z, obtained in the open-aperture experiment at $\varphi = 45°$ and $E_{in} =$ (*1*) 8, (*2*) 22, and (*3*) 84 μJ (symbols are experimental data and the solid lines are approximations by the theoretical functions describing two-photon absorption).

SA and inverse SA in platinum nanoparticle suspensions [29] and in silver nanowire suspensions [40]. In these studies, carried out with nanosecond laser pulses, the spread of the experimental values of normalised transmittance was as large as 1% [29] and 5% [40]. In our opinion, one of the reasons for this large spread of experimental points is the influence of the interference on the transmittance under monochromatic laser pumping.

6. Study of the nonlinear absorption in a colour glass optical filter

The potential of the developed laser system can also be demonstrated by the example of studying the nonlinear absorption in optical filters made of inorganic colour glasses [GOST (State Standard) 9411-81]. Note that colour optical filters are widely used in experiments. Some of these filters exhibit nonlinear optical properties [41]. An example is yellow filters made of colour glass ZhS18, which contain $CdS_{1-x}Se_x$ microcrystallites [42].

Figure 8 presents the transmission spectrum (with respect to air) of a standard 3-mm-thick yellow filter ZhS18, installed at an angle of 45° with respect to the incident light beam. The linear transmittance at a wavelength of 532 nm is 83.2%. The inset in Fig. 8 shows the open-aperture z-scan data for the same filter, oriented at an angle of 45° with respect to the incident laser beam, obtained at different pulse energies. One can observe a large dip in the dependence of transmittance $\overline{T}_{oa}(z)$ in the region of the focused laser beam waist. The transmittance decreases by 6% at a laser pulse energy of 8 μJ (power density 5 MW cm^{-2}) in the waist. It was shown that the experimental dependences $\overline{T}_{ca}(z) = T_{ca}(z)/T_{ca}(z = 70\text{ mm})$ obtained for the optical branch of the closed-aperture scheme almost coincide with the corresponding dependences $\overline{T}_{oa}(z)$. This means that SA and nonlinear refraction do not manifest themselves in the ZhS18 filter under aforementioned experimental conditions. All experimental dependences presented in Fig. 8 (inset) are well approximated by the formulas describing the two-photon absorption [1]. The β value characterising the two-photon absorption in optical filter ZhS18 was found to be 0.13±0.02 cm MW^{-1}, which is an order of magnitude smaller than the nonlinear absorption coefficient in silicate glass doped with copper nanoparticles [43].

7. Conclusions

Thus, applying a narrow laser beam jointly with an uncoated optical cell (inclined with respect to the optical axis) in z-scan measurements under monochromatic pulsed laser pumping, one can obtain dependences of the nonlinear transmittance on intensity with a high accuracy. It was shown that the transmittance can be measured with a spread less than 0.17%. The data making it possible to calculate the nonlinear absorption and nonlinear refraction coefficients of liquid can be obtained in one scan pass. An application of the developed scheme allows one to observe saturable absorption and nonlinear refraction in multiwalled CNT suspensions and investigate the two-photon absorption in colour glass filters. In an aqueous suspension of multiwalled CNTs, saturable absorption can be observed in the pure form at a wavelength of 532 nm and at intensities of about 10 MW cm^{-2}. An increase in intensity by a factor of 2–3 leads to suppression of SA via nonlinear absorption and nonlinear light scattering. The coefficient characterising the two-photon absorption in a yellow optical filter ZhS18 at a wavelength of 532 nm was measured to be 0.13±0.02 cm MW^{-1}.

Acknowledgements. This work was supported by the Russian Foundation for Basic Research (Grant Nos 16-42-180147_r_ural_a and 16-38-0055_mol_a) and the Finnish Academy of Sciences (Grant No. 288547).

References

1. Sheik-Bahae M., Said A.A., Wei T.H., et al. *IEEE J. Quantum Electron*., **26** (4), 760 (1990).
2. Chapple P.B., Staromlynska J., Hermann J.A., et al. *J. Nonlinear Opt. Phys. Mater*., **6** (3), 251 (1997).
3. Vivien L., Anglaret E., Riehl D., et al. *Opt. Commun*., **174**, 271 (2000).
4. Korovin S.B., Orlov A.N., Prokhorov A.M., et al. *Kvantovaya Elektron*., **31** (9), 817 (2001) [*Quantum Electron*., **31** (9), 817 (2001)].
5. Mikheev G.M., Bulatov D.L., Mogileva T.N., et al. *Pis'ma Zh. Tekh. Fiz*., **33** (6), 41 (2007).
6. Mikheev G.M., Kuznetsov V.L., Bulatov D.L., et al. *Kvantovaya Elektron*., **39** (4), 342 (2009) [*Quantum Electron*., **39** (4), 342 (2009)].
7. Vanyukov V.V., Mikheev G.M., Mogileva T.N., et al. *J. Opt. Soc. Am. B*., **31** (12), 2990 (2014).
8. Tereshchenko S.A., Podgaetskii V.M., Gerasimenko A.Yu., et al. *Kvantovaya Elektron*., **45** (4), 315 (2015) [*Quantum Electron.*, **45** (4), 315 (2015)].
9. Ovchinnikov O.V., Smirnov M.S., Perepelitsa A.S., et al. *Kvantovaya Elektron*., **45** (12), 1143 (2015) [*Quantum Electron*., **45** (12), 1143 (2015)].
10. Potamianos D., Papadakis I., Kakkava E., et al. *J. Phys. Chem. C*, **119**, 24614 (2015).
11. Karimzadeh R., Arandian A. *Laser Phys. Lett.*, **12**, 025401 (2015).
12. Van Stryland E.W., Sheik-Bahae M. *Characterization techniques and tabulations for organic nonlinear materials* (New York: Marcel Dekker, 1998).
13. George M., Muneera C.I., Singh C.P., et al. *Opt. Laser Technol*., **40**, 373 (2008).
14. Ferdinandus M.R., Reichert M., Ensley T.R., et al. *Opt. Mater. Express*, **2** (12), 1776 (2012).
15. Tausenev A.V., Obraztsova E.D., Lobach A.S., et al. *Kvantovaya Elektron*., **37** (3), 205 (2007) [*Quantum Electron*., **37** (3), 205 (2007)].
16. Hasan T., Sun Z., Wang F., et al. *Adv. Mater*., **21** (38-39), 3874 (2009).
17. Sun Z., Hasan T., Ferrari A.C. *Phys. E,* **44**, 1082 (2012).
18. Mikheev G.M., Vanyukov V.V., Mogileva T.N., et al. *Pis'ma Zh. Tekh. Fiz*., **41** (24), 9 (2015).
19. Tan W.D., Su C.Y., Knize R.J., et al. *Appl. Phys. Lett*., **96**, 031106 (2010).
20. Rozenberg G.V. *Optika tonkosloinykh pokrytii* (Optics of Thin-Layer Coatings) (Moscow: Fizmatlit, 1958).
21. Mikheev G.M., Maleev D.I., Mogileva T.N. *Kvantovaya Elektron*., **19** (1), 45 (1992) [*Quantum Electron*., **22** (1), 37 (1992)].
22. Krivenkov R.Yu., Mikheev G.M., Zonov R.G., et al. *Khim. Fiz. Mezoskopiya*, **17** (3), 471 (2015).
23. Okotrub A.V., Shevtsov Yu.V., Nasonova L.I., et al. *Prib. Tekh. Eksp*., (1), 193 (1995).
24. Okotrub A.V., Yudanov N.F., Aleksashin V.M., et al. *Vysokomol. Soedin., Ser. A*, **49** (6), 1049 (2007).
25. Mikheev G.M., Vanyukov V.V., Mogileva T.N., Okotrub A.V. *Prib. Tekh. Eksp*., No. 6, 81 (2010).
26. Mikheev G.M., Mogileva T.N., Okotrub A.V., et al. *Kvantovaya Elektron*., **40** (1), 45 (2010) [*Quantum Electron*., **40** (1), 45 (2010)].
27. Dresselhaus M.S., Dresselhaus G., Saito R., Jorio A. *Phys. Rep*., **409**, 47 (2005).
28. Kuznetsov V.L., Bokova-Sirosh S.N., Moseenkov S.I., et al. *Phys. Status Solidi B*, **251**, 2444 (2014).
29. Gao Y., Zhang X., Li Y., et al. *Opt. Commun*., **251**, 429 (2005).
30. Ganeev R.A., Usmanov T. *Kvantovaya Elektron*., **37** (7), 605 (2007) [*Quantum Electron.*, **37** (7), 605 (2007)].
31. Vanyukov V., Mogileva T., Mikheev G., et al. *Appl. Opt*., **52** (18), 4123 (2013).
32. Sakakibara Y., Tatsuura S., Kataura H., et al. *Jpn. J. Appl. Phys*., **42**, L494 (2003).
33. Set S.Y., Yaguchi H., Tanaka Y., Jablonski M. *J. Light Technol.*, **22** (1), 51 (2004).
34. Il'ichev N.N., Obraztsova E.D., Garnov S.V., Mosaleva S.E. *Kvantovaya Elektron.*, **34** (6), 572 (2004) [*Quantum Electron*., **34** (6), 572 (2004)].
35. Il'ichev N.N., Obraztsova E.D., Pashinin P.P., et al. *Kvantovaya Elektron*., **34** (9), 785 (2004) [*Quantum Electron*., **34** (9), 785 (2004)].
36. Lim S., Elim H., Gao X., et al. *Phys. Rev. B*., **73**, 0455402 (2006).
37. Lin X.C., Zhang L., Tsang Y.H., et al. *Laser Phys. Lett*., **10**, 055805 (2013).
38. Battaglin G., Calvelli P., Cattaruzza E., et al. *Appl. Phys. Lett*., **78**, 3953 (2001).
39. Ganeev R.A., Ryasnyansky A.I., Baba M., et al. *Appl. Phys. B*, **78**, 433 (2004).
40. Zheng C., Ye X.Y., Cai S.G., et al. *Appl. Phys. B*, **101**, 835 (2010).
41. Bindra K.S., Chari R., Shukla V., et al. *J. Opt. A: Pure Appl. Opt.*, **1**, 73 (1999).
42. Bondar' I.V., Zyul'kov V.A., Kotov S.G., et al. RF Patent No. 1797963, *Bull. Izobret.*, No. 2 (1993).
43. Ganeev R.A., Ryasnyanskii A.I., Stepanov A.L., Usmanov T. *Kvantovaya Elektron.*, **33**, 1081 (2003) [*Quantum Electron*., **33**, 1081 (2003)].